

# Journal Pre-proof

The bZIP transcription factor RISBZ1 balances grain filling and ER stress response in rice grains

Qi Sun, Erchao Duan, Ruonan Jing, Yulong Ren, Huan Xu, Chuanwei Gu, Wenting Lv, Xiaokang Jiang, Rongbo Chen, Qingkai Wang, Yipeng Zhang, Rushuang Zhang, Hongyi Xu, Yunpeng Zhang, Jiajia Chi, Yunfei Fu, Yun Zhu, Yu Zhang, Binglei Zhang, Xuan Teng, Hui Dong, Xue Yang, Lei Zhou, Yunlu Tian, Xi Liu, Shijia Liu, Xiuping Guo, Cailin Lei, Ling Jiang, Yihua Wang, Jianmin Wan

PII: S2590-3462(25)00220-2

DOI: <https://doi.org/10.1016/j.xplc.2025.101458>

Reference: XPLC 101458

To appear in: *PLANT COMMUNICATIONS*

Received Date: 18 February 2025

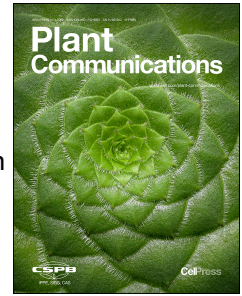
Revised Date: 29 June 2025

Accepted Date: 14 July 2025

Please cite this article as: Sun, Q., Duan, E., Jing, R., Ren, Y., Xu, H., Gu, C., Lv, W., Jiang, X., Chen, R., Wang, Q., Zhang, Y., Zhang, R., Xu, H., Zhang, Y., Chi, J., Fu, Y., Zhu, Y., Zhang, Y., Zhang, B., Teng, X., Dong, H., Yang, X., Zhou, L., Tian, Y., Liu, X., Liu, S., Guo, X., Lei, C., Jiang, L., Wang, Y., Wan, J., The bZIP transcription factor RISBZ1 balances grain filling and ER stress response in rice grains, *Plant Communications* (2025), doi: <https://doi.org/10.1016/j.xplc.2025.101458>.

This is a PDF file of an article that has undergone enhancements after acceptance, such as the addition of a cover page and metadata, and formatting for readability, but it is not yet the definitive version of record. This version will undergo additional copyediting, typesetting and review before it is published in its final form, but we are providing this version to give early visibility of the article. Please note that, during the production process, errors may be discovered which could affect the content, and all legal disclaimers that apply to the journal pertain.

© 2025 The Author(s). Published by Elsevier Inc. on behalf of CAS Center for Excellence in Molecular Plant Sciences, Chinese Academy of Sciences, and Chinese Society for Plant Biology.



## The bZIP transcription factor RISBZ1 balances grain filling and ER stress response in rice grains

Qi Sun<sup>1,3</sup>, Erchao Duan<sup>2,3</sup>, Ruonan Jing<sup>2,3</sup>, Yulong Ren<sup>1,3</sup>, Huan Xu<sup>2</sup>, Chuanwei Gu<sup>2</sup>, Wenting Lv<sup>2</sup>, Xiaokang Jiang<sup>2</sup>, Rongbo Chen<sup>2</sup>, Qingkai Wang<sup>2</sup>, Yipeng Zhang<sup>2</sup>, Rushuang Zhang<sup>2</sup>, Hongyi Xu<sup>2</sup>, Yunpeng Zhang<sup>2</sup>, Jiajia Chi<sup>2</sup>, Yunfei Fu<sup>2</sup>, Yun Zhu<sup>1</sup>, Yu Zhang<sup>2</sup>, Binglei Zhang<sup>2</sup>, Xuan Teng<sup>2</sup>, Hui Dong<sup>2</sup>, Xue Yang<sup>2</sup>, Lei Zhou<sup>2</sup>, Yunlu Tian<sup>2</sup>, Xi Liu<sup>2</sup>, Shijia Liu<sup>2</sup>, Xiuping Guo<sup>1</sup>, Cailin Lei<sup>1</sup>, Ling Jiang<sup>2</sup>, Yihua Wang<sup>2,\*</sup> and Jianmin Wan<sup>1,2,\*</sup>

1 State Key Laboratory of Crop Gene Resources and Breeding, National Key Facility for Crop Gene Resources and Genetic Improvement, Institute of Crop Sciences, Chinese Academy of Agricultural Sciences, Beijing, 100081, China

2 State Key Laboratory of Crop Genetics & Germplasm Enhancement and Utilization, Zhongshan Biological Breeding Laboratory, Jiangsu Nanjing Rice Germplasm Resources National Field Observation and Research Station, Nanjing Agricultural University, Nanjing, 210095, China

<sup>3</sup>These authors contributed equally to this work.

\*To whom correspondence may be addressed: Jianmin Wan (wanjianmin@caas.cn or wanjm@njau.edu.cn); Yihua Wang (yihuawang@njau.edu.cn).

**Running title:** RISBZ1 balances ER stress and grain filling

**Summary:** *RISBZ1* mutation results in defective grain-filling and serious ER stress. *RISBZ1* interacts with bZIP50 and bZIP60 to suppress the overactivation of UPR at the cost of downregulating the transcription of starch and storage protein synthesis genes normally regulated by *RISBZ1*. Therefore, *RISBZ1* plays a critical role in maintaining a balance between storage reserve accumulation and ER stress under adverse conditions.

## ABSTRACT

In cereal crops, the endosperm is responsible for synthesizing large amounts of proteins, including storage proteins and functional factors essential for the accumulation of storage substances. The unfolded protein response (UPR) monitors the folding of nascent polypeptides in the endoplasmic reticulum (ER) to alleviate cellular stress. However, the molecular mechanisms linking UPR to endosperm development in plants remain poorly understood. In this study, we isolated and characterized a rice (*Oryza sativa* L) mutant with defective endosperm development, which we named *floury endosperm27* (*flo27*). Molecular cloning revealed that *FLO27* encodes RISBZ1/bZIP58, an endosperm-specific transcription factor that is co-expressed with seed storage protein (SSP) genes and starch biosynthesis-related genes in rice. We found that the *flo27* mutant exhibits severe ER stress, accompanied by the upregulation of UPR-related genes. Notably, RISBZ1 interacts with bZIP50 and bZIP60 to antagonistically downregulate the expression of downstream UPR genes. These interactions simultaneously suppress the expression of SSP genes and starch biosynthesis-related genes, ultimately leading to reduced dry matter accumulation. In conclusion, our findings demonstrate that RISBZ1 acts as a “brake signal” to mitigate ER stress, thereby broadening our understanding of the delicate trade-off between grain-filling and adaptation to adverse environmental conditions in rice.

**Key words:** Endosperm development, unfolded protein response, RISBZ1, bZIP50, bZIP60

## INTRODUCTION

In eukaryotic cells, endoplasmic reticulum (ER) is the site of synthesis and folding of membrane and secretory proteins, which represent a large portion of the total protein output (Lin et al., 2008). These proteins are properly folded and modified in the ER lumen before being transferred to their functional destinations. The biosynthetic capacity of the ER can be overwhelmed under biotic and abiotic stresses (e.g., pathogen attack, heat stress) or in developmental states requiring elevated secretory protein biosynthesis (e.g., cell growth). ER stress is a potentially fatal condition that occurs when misfolded and unfolded proteins accumulate in the ER (Ron et al., 2007; Vitale et al., 2008; Liu et al., 2010b). To alleviate ER stress, cells trigger a

sophisticated signaling pathway known as the unfolded protein response (UPR), which modulates gene expression and restores ER homeostasis by enhancing the ER's protein-folding ability and by removing misfolded/unfolded proteins through ER quality control and the ER-associated protein degradation (ERAD) pathway (Harding et al., 1999).

Recently, molecular genetic studies have started to unravel the mechanisms regulating the UPR in plants. Two UPR signaling pathways have been identified: one mediated by the inositol-requiring enzyme (IRE1)-bZIP60 module, which is the plant counterpart of the animal IRE1-XBP1 pathway and the other mediated by site-1/site-2 proteases (S1P/S2P)-bZIP17/bZIP28, which is the plant counterpart of the animal Activating Transcription Factor 6 (ATF6) pathway (Liu et al., 2007a, 2007b; Gao et al., 2008; Liu et al., 2010a; Deng et al., 2011; Nagashima et al., 2011). *Arabidopsis thaliana* bZIP60 (*AtbZIP60*) is a transcription factor normally anchored to the ER membrane (Iwata et al., 2005). Upon ER stress, IRE1 splices the mRNA of *AtbZIP60*, resulting in a frameshift and production of a newly translated *AtbZIP60* without any obvious transmembrane domain, which is then translocated to the nucleus to regulate the expression of downstream genes (Deng et al., 2011). Although *AtbZIP60* is conservatively regulated by cytoplasmic splicing, some of its properties are significantly different from those of HAC1 and XBP1 (Iwata et al., 2012). A unique feature in *AtbZIP60* is the presence of a transactivation domain at its N-terminus (Iwata et al., 2009), in contrast to yeast HAC1 and animal XBP1, the transactivation domains appear at their C-terminus only after splicing. Notably, the two IRE1 homologues in animals have distinct functions (Bertolotti et al., 2001; Iwawaki et al., 2001). While *AtIRE1A* and *AtIRE1B* share functional redundancy in ER stress response, the *AtIRE1C* represents an unconventional isoform that lacks a luminal domain and involved in the regulation of gametogenesis in *Arabidopsis* (Nakamura et al., 2011; Pu et al., 2019). Similar to ATF6, *AtbZIP28* is a type II transmembrane protein, with its N-terminal bZIP domain oriented toward the cytoplasm and the C-terminus located in the ER lumen. Normally, *AtbZIP28* is located on the ER. Under ER stress, however, *AtbZIP28* is transported to the Golgi, where it is hydrolyzed by Golgi-localized *AtS1P* and *AtS2P*, and then translocated to the nucleus to regulate the expression of downstream genes

(Howell, 2013). Notably, AtbZIP17 and AtbZIP28 share similar protein structures, domains and S1P proteolytic sites. The UPR pathways are well conserved in rice (*Oryza sativa*) (Zhou et al., 2022). In brief, OsbZIP50 is the rice ortholog of AtbZIP60, and is activated by OsIRE1-dependent mRNA unconventional splicing (Hayashi et al., 2012; Lu et al., 2012). OsbZIP60 is the ortholog of AtbZIP28 in rice, which is activated presumably through proteolysis (Hayashi et al., 2013).

Given the importance of the UPR in maintaining cellular homeostasis, a strict monitoring system must regulate its magnitude and duration. Thus, the mechanisms regulating the UPR are crucial for plant survival. While most studies to date have focused on how the UPR is activated, information on how it is attenuated to ensure cell viability is limited. To date, several UPR “brake” genes have been identified, including yeast *Snf1* (Mizuno et al., 2015), metazoan *Wolfram syndrome 1 (WFS1)* (Fonseca et al., 2010), and Arabidopsis *NON-EXPRESSOR OF PATHOGENESIS-RELATED GENES1 (NPR1)* (Lai et al., 2018), *BLISTER (BLI)* (Hong et al., 2019), *CONSTITUTIVE EXPRESSION OF PATHOGENESIS-RELATED GENES5 (CPR5)* (Meng et al., 2017), and *ELONGATED HYPOCOTYL 5 (HY5)* (Nawkar et al., 2017). However, despite this progress, the mechanisms underlying UPR regulation remain largely unknown, especially in rice, a staple food for more than half of the global population.

Rice seeds accumulate copious starch and storage proteins during grain filling. In addition to starch biosynthesis-related proteins and seed storage proteins (SSPs), numerous transcription factors play important roles in this process, such as RICE SEED bZIP1 (RISBZ1), Rice Prolamin-box binding factor (RPBF) and OsNAC20/26 (Onodera et al., 2001; Kawakatsu et al., 2009; Wang et al., 2020). The rice basic leucine zipper factor RISBZ1 (also known as OsbZIP58) regulates the biosynthesis of SSPs and starch by directly binding the GCN4 and ACGT motifs, respectively, in the promoters of storage-related genes (Onodera et al., 2001; Wang et al., 2013). As an ortholog of RISBZ1 in maize, the famous Opaque2 (O2) protein is also a key transcription factor for storage reserve accumulation during seed development (Qiao et al., 2016; Zhang et al., 2016; Deng et al., 2020; Li et al., 2020; Chen et al., 2023). To synthesize these large amounts of storage reserves,

endosperm cells must maintain a certain level of chaperones to ensure proper protein folding. However, when ER stress occurs, such as under the high temperatures frequently encountered during grain filling, these chaperones may be overwhelmed in the endosperm. Therefore, the mechanism by which rice endosperm coordinates dry matter accumulation (grain filling) with precise regulation of the UPR remains to be addressed.

Here, we identified and characterized the role of RISBZ1/bZIP58 in UPR signaling during rice endosperm development. We found that mutation of RISBZ1 results in significant up-regulation of UPR downstream genes. RISBZ1 indirectly regulates UPR-related downstream genes under ER stress by interacting with bZIP50 and bZIP60 to repress their DNA binding activities. Notably, these interactions compromise the expression of SSP genes and starch biosynthesis-related genes to reduce dry matter accumulation. Taken together, our results highlight the key role of RISBZ1 in alleviating ER stress and provide new insights into the coordination of the ER stress and dry matter accumulation during seed development in rice.

## RESULTS

### Compromised reserve accumulation in the *flo27* grain

To identify key factors for endosperm development in rice, we screened for mutants with altered endosperm characteristics. The *floury endosperm27* (*flo27*) mutant was isolated from a T-DNA mutant pool generated from rice (*Oryza sativa*) ssp. *japonica* cv. Dongjin. Plant growth and development are comparable between *flo27* and Dongjin during the vegetative stage. At the heading stage, the plant height of *flo27* was slightly reduced, but with similar tiller number and panicle length, compared to the wild type (Dongjin) (Supplemental Figures 1A-1D). During grain developmental stage, *flo27* exhibited a significantly lower grain-filling rate than Dongjin, leading to partially opaque mature endosperm with a shrunken and floury-white belly that occupies the central to ventral region of the seed (Figures 1A-1D; Supplemental Figure 1E). Scanning electron microscopic (SEM) observation showed that starch granules in mature endosperm of *flo27* were round and loosely packed in the floury-white belly, in contrast to the regular and compact crystal structure observed in Dongjin (Figures 1E-1H).

Further semithin section observation of the developing endosperm at 12 days after flowering (DAF) revealed that the endosperm cells of Dongjin contained compound starch grains (SGs), consisting of several dozens of polyhedral and sharp-edged granules (Figure 1I). While in the opaque parts of *flo27*, smaller and scattered single SGs were obviously observed in the cytosol (Figure 1J). In addition, ultrathin section observation of 12 DAF developing endosperm showed that the compact, irregular-shaped protein body II (PBII, mainly consists of glutelins and  $\alpha$ -globulin), as well as round-shaped PBI (mainly accumulates prolamins) were readily observed in the endosperm cells of Dongjin (Figure 1K). However, most of the PBIIs in *flo27* were partially empty compared to the fully-filled PBIIs in wild type (Figure 1L), reflecting the reduced storage protein accumulation in *flo27*. Consistent with the defected filling of starch granules and protein bodies, *flo27* seeds also displayed decreased contents of total starch, amylose and protein (Supplemental Figures 1F-1H). Accordingly, RT-qPCR analysis showed that the expression levels of numerous genes involved in starch and storage protein biosynthesis were significantly downregulated in *flo27* endosperm (Supplemental Figure 2A). Moreover, immunoblot analysis also revealed the dramatically reduced abundances of AGPL2, AGPS2a, BEI, SSI, GluA and GluB as well as slightly decreased levels of ISAI, BEIIb, GBSSI and Glb in *flo27* (Supplemental Figure 2B), further validating the compromised accumulation of starch and storage proteins. Due to the diminished grain filling, the grain length, grain width and especially grain thickness were significantly reduced for *flo27*, leading to a dramatic decrease in grain weight (Supplemental Figures 1I-1M). Taken together, these phenotypic and molecular characterization results indicated the crucial role of *FLO27* in proper endosperm development in rice.

To clone the gene responsible for the *flo27* phenotypes, an F<sub>2</sub> population was generated by crossing the *flo27* mutant with *indica* cv. N22. Twenty-two grains with the opaque phenotype were selected from the segregating population for linkage analysis. The gene was initially localized to a 17.5-cM region on the short arm of chromosome 7. Subsequent fine-mapping using 1464 recessive individuals restricted the locus to a 253-kb region between markers BS-4 and BS-5 that covered three BACs, OJ1361\_E02, OJ1014\_E09,

and OJ1506\_G02. 18 open reading frames (ORFs) in this region were predicted by the Rice Expression Profile Database (<http://ricexpro.dna.affrc.go.jp/>) (Supplemental Figure 3A). Sequence analysis only revealed a 188-bp insertion in the last exon of *ORF13* (*LOC\_Os07g08420*), resulting in a frameshift and premature translation termination (Figure 1M). No sequence alterations were found in other ORFs. For the complementation test, we transformed a construct containing the 2-kb promoter region and coding sequence of *ORF13* into calli of *flo27*. Grains of the positive transgenic plants (Com) showed restoration of the defective endosperm phenotype to a Dongjin-like appearance, along with Dongjin-like protein levels (Figures 1N and 1O). Furthermore, we generated two *ORF13* knockout lines using the clustered regularly interspaced short palindromic repeats (CRISPR)/Cas9 approach, and both mutants displayed opaque floury endosperm phenotypes reminiscent of *flo27* (Supplemental Figures 3B-3D). Thus, these genetic data validated that *ORF13* is the causative gene for endosperm defect in the *flo27* mutant.

#### ***RISBZ1* mutation results in severe ER stress in developing endosperm**

*ORF13* encodes the bZIP transcription factor *RISBZ1*/bZIP58, an ortholog of maize Opaque2 (O2). To determine which molecular pathways were potentially disrupted in *flo27* leading to aberrant endosperm development, we conducted RNA-seq analysis on developing endosperm from *flo27* and Dongjin collected at 14 DAF. Compared to Dongjin, 384 genes were up-regulated ( $\log_2$  fold change > 1) and 314 genes were down-regulated ( $\log_2$  fold change < -1) in *flo27* (FDR < 0.05) (Supplemental Figure 4). In line with the altered starch and storage protein accumulation in *flo27*, many of these differentially expressed genes (DEGs) were related to the biosynthesis of storage proteins and starch (Dataset S1). Intriguingly, Kyoto Encyclopedia of Genes and Genomes (KEGG) and Gene Ontology (GO) analysis further suggested that many DEGs were also significantly enriched for the protein processing in endoplasmic reticulum pathway and the unfolded protein binding as well as heat shock protein binding functions, implying the possible involvement of *RISBZ1* in the UPR (Figures 2A and 2B; Dataset S1). Further RT-qPCR analysis confirmed the increased expression levels of multiple UPR genes in the *flo27* endosperm, such as protein disulfide isomerase-like

enzymes (*PDILs*), binding proteins (*BiPs*), heat shock proteins (*HSPs*), calreticulin (*CRT*), calnexin (*CNX*), ER-localized DnaJ family member 3 (*ERDJ3*), nucleotide exchange factor (*NEF*), UDP-glucose transferase 4 (*UGT4*), membrane-associated bZIP transcription factors (*bZIP50*, *bZIP39* and *bZIP60*), ERAD-related protein (*Derlin*) and the programmed cell death (PCD) marker (*NPR1*) (Figures 2C-2F). Moreover, immunoblot analysis revealed an increased accumulation of ER stress-related proteins BiP1 and PDIL1-1 in 14-DAF *flo27* endosperm at the protein level (Figure 2G). Notably, the accumulations of BiP1 and PDIL1-1 were recovered to the wild-type levels in developing grains of the complemented lines (Com) (Supplemental Figure 5). Moreover, the unconventional splicing of *bZIP50* mRNA (*bZIP50s*) was obviously elevated in endosperm cells of *flo27*, which is not occurred in Dongjin (Supplemental Figure 6), further supporting the involvement of *RISBZ1* in the UPR during rice endosperm development.

Opaque2 (*O2*), the counterpart of *RISBZ1* in maize, is also a key transcription factor involved in storage reserve accumulation during seed development (Qiao et al., 2016; Zhang et al., 2016; Deng et al., 2020; Li et al., 2020; Chen et al., 2023). In addition, *O2* has been reported to affect the expression of *Heat shock protein (Hsp)* family genes (Guo et al., 2012), which are generally associated with heat stress and UPR (Yu et al., 2015). To determine whether *O2* plays a similar role in regulating UPR in maize, we performed RT-qPCR analysis using developing maize grains from WT and the *opaque2 (o2)* mutant. Our results revealed that only a few ER stress-related genes were slightly upregulated, while the majority were unchanged or even significantly decreased (Supplemental Figure 7). These findings indicate that the expression patterns of UPR-related genes in maize differ significantly from those in rice, implying possible functional divergence between *Opaque2* and *RISBZ1*, or species-specific differences underlying endosperm development between rice and maize.

### ***RISBZ1* physically interacts with *bZIP50* and *bZIP60* during ER stress**

Rice *bZIP50* and *bZIP60*, orthologs of *AtbZIP60* and *AtbZIP28*, respectively, are key bZIP transcription factors that function as transducers of ER stress signaling (Hayashi et al., 2012; Cao et al., 2022; Yang et al., 2022). In our RT-qPCR analysis, the expression levels of both *bZIP50* and *bZIP60* were

significantly up-regulated in *flo27* (Figure 2E). Given the involvement of RISBZ1 in regulating ER stress and its role as a typical bZIP transcription factor, we aimed to identify the possible interactions between RISBZ1, bZIP50 and bZIP60.

We firstly examined their subcellular localization by transient expression assays in rice leaf sheath protoplasts under both normal and ER stress conditions induced by 10 mM dithiothreitol (DTT), a known ER stress inducer. The results showed that RISBZ1 localized to the nucleus under both conditions (Supplemental Figure 8). Furthermore, GFP fluorescence of bZIP50-GFP and GFP-bZIP60 overlapped well with the red fluorescence of the mCherry-KDEL ER marker under normal conditions (Figure 3A). However, after DTT treatment to induce ER stress, both bZIP50 and bZIP60 proteins translocated to the nucleus (Figure 3A), implying that they undergo the ER-to-nucleus relocation in response to ER stress. Consistent with these results, bZIP50 and bZIP60 showed a typical ER localization pattern in protoplasts from Dongjin, whereas in *flo27*, both proteins mainly localized to the nucleus in response to the intrinsic ER stress condition (Figure 3A; Supplemental Figure 9). Therefore, we hypothesized that RISBZ1 might interact with bZIP50 and bZIP60 in the nucleus under ER stress conditions.

Indeed, yeast two-hybrid (Y2H) assays confirmed the physical interaction between RISBZ1 and bZIP50 or bZIP60 (Figure 3B). *In vitro* pull-down assays further validated the direct interaction of RISBZ1 with both bZIP50 and bZIP60 proteins (Figure 3C). To confirm these interactions *in vivo*, we performed luciferase complementation imaging (LCI) and bimolecular fluorescence complementation (BiFC) assays with 2 mM DTT treatment. These assays demonstrated the interactions only occurred upon DTT treatment (Figures 3D and 3E). Thus, the ER stress-triggered translocation of bZIP50 and bZIP60 to the nucleus and their interaction with RISBZ1 further suggest an important role of RISBZ1-bZIP50/60 complex formation in the UPR regulation.

### **bZIP50 and bZIP60 directly regulate UPR downstream genes**

To further determine whether bZIP50 and bZIP60 are directly involved in the UPR, knockout mutants of both genes were generated using the CRISPR/Cas9 system (Supplemental Figures 10A and 10B). Notably, the mature grains of *bZIP50* knockout lines (*bzip50*) exhibited only slight

chalkiness, while *bZIP60* knockout lines (*bzip60*) displayed a floury phenotype similar to that of *flo27* (Supplemental Figures 10C and 10D). RT-qPCR analysis of 14 DAF developing endosperm revealed that *PDIL1-1*, *PDIL2-2*, *PDIL5-3*, *PDIL5-4* and *ERDJ3* were down-regulated, while *PDIL1-4*, *PDIL2-1*, *PDIL2-3* and *BiP-1* were up-regulated in *bzip50* (Figure 4A). In contrast, expression levels of all UPR downstream genes tested were up-regulated in the endosperm of *bzip60* (Figure 4C). Further immunoblotting showed that the levels of representative ER stress-related proteins, such as BiP1 and PDIL1-1, were slightly increased in *bzip50* endosperm, but markedly elevated in the *bzip60* mutant (Figures 4B and 4D). These genetic and molecular data suggest that mutation of *bzip60* leads to disrupted ER homeostasis and a subsequent unfolded protein response in rice endosperm, ultimately resulting in defects of endosperm development.

We next sought to determine whether bZIP50 and bZIP60 could directly target the promoter regions of various UPR genes by performing Y1H assays. Our results showed that bZIP60 directly bound to the promoters of *CRT*, *PDIL1-4*, *PDIL2-1*, *PDIL2-3*, *ERDJ3*, *BiP1* and *NEF*, while bZIP50 was recruited to the promoter regions of *PDIL1-4*, *PDIL2-1*, *PDIL2-3* and *NEF* (Figure 4E). These findings suggest that bZIP50 and bZIP60 directly regulate transcription of these UPR-related genes. To further confirm above results, luciferase (LUC) activity assays were performed, demonstrating that both bZIP50 and bZIP60 activated transcription of luciferase driven by the *PDIL1-4* and *NEF* promoters (Figures 4F and 4G). Overall, these results further support that bZIP50 and bZIP60 participate in the UPR by directly regulating the transcription of UPR-related genes.

### **RISBZ1 and bZIP50/60 repress the transcriptional activity of each other**

Our RT-qPCR analysis showed that *RISBZ1* mutation led to significant up-regulation of numerous ER stress/UPR-related genes in *flo27* (Figure 2), and the physical interaction of RISBZ1 with bZIP50 and bZIP60, two typical transducers of ER stress signaling (Figure 3), suggests that RISBZ1 may function as a repressor of the UPR signaling. Since grains of the *bZIP60* knockout lines also exhibit obviously elevated expression of all UPR-related genes tested and the floury endosperm phenotype similar to that of *flo27* (Figure 4), we thus performed transient dual-LUC assay in rice protoplasts to

evaluate the transcriptional regulatory relationship between RISBZ1 and bZIP60. As shown in Fig 5A and 5B, bZIP60 alone enhanced the expression of luciferase reporter gene driven by the *BiP1* and *PDIL1-1* promoters. However, when co-expressed with *RISBZ1*, the transcriptional activation activity of bZIP60 was significantly attenuated. To test whether RISBZ1 affects the DNA binding affinity of bZIP60, an *in vitro* electrophoresis mobility shift assay (EMSA) was performed. bZIP60 could directly bind to the ER stress response elements (ERSEs) in the promoter regions of *BiP1* and *PDIL1-1*, and no obvious shifted bands were observed for RISBZ1, indicating a lack of binding to these motifs (Figures 5C and 5D). However, the presence of increasing amounts of RISBZ1 in the reactions significantly reduced the binding ability of bZIP60 to the target probes, indicating that RISBZ1 interferes with the DNA binding ability of bZIP60 (Figures 5C and 5D), thus alleviating the UPR response mediated by bZIP60.

Moreover, we also tested the reverse regulatory effects of bZIP50/60 on the transcriptional activity of RISBZ1 for storage protein and starch synthesis. RISBZ1 alone could substantially enhance the transcription of *GluA2* and *AGPL3* (Figures 5E and 5F). However, the transcriptional activation activity of RISBZ1 was significantly compromised when co-expressed with bZIP50/60 (Figures 5E and 5F). Further EMSA demonstrated that the bZIP50/60-RISBZ1 complex formation could also interfere with the DNA binding ability of RISBZ1 to the target probes (Figures 5G-5J), similar to the effect of RISBZ1 on bZIP50/60 activity. To illustrate the biological function of bZIP50/60-RISBZ1 complex formation *in vivo*, the bZIP60-specific polyclonal antibodies were generated (Supplemental Figure 11). ChIP-qPCR analysis verified that bZIP60 was significantly enriched in the promoter regions of downstream UPR-related genes, such as *BiP1*, *PDIL1-1*, *PDIL1-4*, *PDIL2-1*, *PDIL2-3*, *NEF* and *CRT* in the *flo27* background, which may ultimately lead to the upregulated UPR in endosperm of *flo27* (Figure 5K).

### **RISBZ1 negatively regulates the UPR during ER stress**

We found that the expression level of *RISBZ1* was significantly upregulated in developing grains of *bzip60* (Figure 6A), suggesting that *RISBZ1* likely responds to ER stress at the transcription level. To further investigate the biological significance of RISBZ1 in ER stress, we overexpressed *RISBZ1* in

isolated rice protoplasts treated with 10 mM DTT to access its regulatory role in ER stress *in vivo*. Our analysis revealed that the expression levels of all tested UPR-related genes were significantly down-regulated (Figures 6B). We also attempted to overexpress the *RISBZ1* coding sequence using both the *CaMV35S* and *Ubiquitin* promoters in the Dongjin variety, but for unknown reasons, none of the transgenic lines showed a significant increase in *RISBZ1* expression levels. Consequently, we generated the double knockout mutants of *bZIP50* and *RISBZ1* (*bzip50 risbz1*) as well as *bZIP60* and *RISBZ1* (*bzip60 risbz1*) (Figures 6C and 6D). Phenotypic analysis demonstrated that grains of both *bzip50 risbz1* and *bzip60 risbz1* double mutants exhibited a more severe floury phenotype, significantly increased grain chalkiness, and reduced grain filling and weight compared to the respective *bzip50* or *bzip60* single mutants (Figures 6C-6H; Supplemental Figure 12). Moreover, the accumulation of ER stress-responsive proteins BiP1 and PDIL1-1 was clearly enhanced in both double mutants, indicating an exacerbated UPR in the endosperm of these mutant lines (Figures 6I and 6J).

Adverse conditions, such as high temperature during grain-filling, are known to induce ER stress. Under normal-temperature conditions (28°C, 12 h light / 22°C, 12 h dark), grains of *bzip50 risbz1* and *bzip60 risbz1* double mutants exhibited mild chalkiness. However, when transferred to high-temperature conditions (35°C, 12 h light / 28°C, 12 h dark), chalkiness degree of the mature grains of Dongjin were significantly increased but with similar grain size. In contrast, the *bzip50* and *bzip60* single mutants displayed a floury phenotype with slightly smaller grains, while the grains of the *bzip50 risbz1* and *bzip60 risbz1* double mutants were strikingly more floury and shrunken, with a marked reduction in grain size (Supplemental Figure 13A). SDS-PAGE analysis showed that proglutelin accumulation in mature grains of *bzip50 risbz1* and *bzip60 risbz1* double mutants was more sensitive to high temperature than in the *bzip50* and *bzip60* single mutants (Supplemental Figure 13B), indicating a disturbance in storage protein biosynthesis and accumulation. Moreover, immunoblot analysis showed that the BiP1 and PDIL1-1 proteins were significantly upregulated in grains of *bzip50*, *bzip60*, *bzip50 risbz1* and *bzip60 risbz1* mutants in response to high temperature (Supplemental Figure 13C), implying that high-temperature conditions

aggravate ER stress and result in the more pronounced abnormalities in grain development in the *bzip50 risbz1* and *bzip60 risbz1* double mutants.

### ***RISBZ1* is selected during *japonica* and *indica* rice domestication**

To determine whether *RISBZ1* underwent selection during rice domestication, we downloaded and compared the SNP variants within the *RISBZ1* genomic region from 115 wild rice accessions (*O. rufipogon* and *O. nivara*), 673 landraces and 995 modern cultivars. SNPs located within the 2 kb upstream region and missense variants in exons were selected for haplotype analysis. Our results identified seven *RISBZ1* haplotypes in wild rice, among which *RISBZ1*-Hap1 and *RISBZ1*-Hap5 are the most common. While in landraces and modern cultivars, *RISBZ1*-Hap2 and *RISBZ1*-Hap6 became the predominant haplotypes in *japonica* and *indica* rice, respectively, each accounting for more than 92% of the accessions (Supplemental Figure 14 A and B). These findings suggest that *RISBZ1* was a selective target during rice domestication.

Further, we validated the selection at the sequence level using population differentiation ( $F_{ST}$ ), nucleotide diversity ( $\pi$ ) and  $\pi$  ratio values. Sequence comparison based on  $F_{ST}$  revealed a clear differentiation in the *RISBZ1* region between wild rice and both *indica* and *japonica*. The  $\pi$  values of both *japonica* and *indica* subpopulations were significantly lower than that in wild rice, leading to higher  $\pi$  ratios compared to the wild rice (Supplemental Figure 14C). Geographic distribution analysis showed that *RISBZ1*-Hap2 accessions are mainly found in Northern China and Japan, whereas *RISBZ1*-Hap6 accessions are mainly distributed in Southern China, India, and other low-latitude areas (Supplemental Figure 14D). Taken together, these results suggest that *RISBZ1*-Hap2 and *RISBZ1*-Hap6 have been subject to positive selection in the *japonica* and *indica* subpopulations, respectively, which may have played important roles in facilitating regional adaptation during rice domestication and improvement.

## **DISCUSSION**

The UPR plays a crucial role in maintaining cellular homeostasis, which is essential for plant growth and development. It is plausible that both the activation and suppression of the UPR must be tightly regulated. While most current studies focus on the activation of the UPR, the mechanisms by which the UPR is suppressed once homeostasis has been disturbed remain poorly understood. To date, only a few UPR-suppression proteins have been

identified. For example, yeast Snf1, an AMP-activated protein kinase (AMPK), is involved in the negative regulation of UPR signaling through the Hog1 MAPK cascade (Mizuno et al., 2015). The metazoan protein Wolfram syndrome 1 (WFS1) physically interacts with ATF6 $\alpha$  and promotes proteasome-mediated degradation, thereby suppressing ATF6 $\alpha$ -mediated signaling in the UPR (Fonseca et al., 2010). In Arabidopsis, NPR1 relocates to nucleus upon ER stress to interact with bZIP60 and bZIP28, causing their transcriptional deactivation (Lai et al., 2018), while BLISTER (BLI) represses IRE1A/IRE1B function under normal growth conditions (Hong et al., 2019). Furthermore, Arabidopsis CPR5 interacts with bZIP60 and bZIP28 to manage the trade-off between plant growth and SA-modulated UPR signaling (Meng et al., 2017). Moreover, HY5 also negatively regulates the UPR by competing with bZIP28 for binding to the G-box-like sequence within the ER stress response element (ERSE) (Nawkar et al., 2017). However, knowledge about the precise regulation of UPR signaling in rice is still limited, particularly during the grain-filling process. How grain filling is coordinated with UPR signaling under stress conditions remains to be elucidated.

RISBZ1 co-expresses with rice seed storage protein genes and activates their transcription in transient expression assays (Onodera et al., 2001; Yamamoto et al., 2006). RISBZ1 also binds to the promoters of multiple rice starch biosynthesis genes *in vivo* (Wang et al., 2013). In addition, RISBZ1 interacts with OsLOL1 to influence gibberellic acid (GA) biosynthesis through the activation of OsKO2, thereby stimulating aleurone PCD and seed germination (Wu et al., 2014). Moreover, rice varieties with lower thermal sensitivity showed reduced alternative splicing of *RISBZ1* mRNA, indicating that RISBZ1 is a heat tolerance factor involved in regulating storage material accumulation under high temperature conditions (Xu et al., 2020). In this study, we found that the *flo27* mutant exhibited floury mature endosperm with abnormal deposition of starch and storage proteins (Figure 1). These results confirmed that RISBZ1 plays a crucial role in dry matter accumulation during rice endosperm development. Besides, we revealed the expression levels of UPR downstream genes were significantly increased in *flo27* (Figure 2), suggesting that severe UPR occurred when *RISBZ1* was mutated. This may also contribute to the defective phenotypes of mature endosperm of *flo27* as it

has been reported the ER stress/UPR activation promotes the formation of grain chalkiness in rice (Bertolotti et al., 2001; Oono et al., 2010; Guo et al., 2012; Han et al., 2012).

As a transcription factor, the induction of numerous UPR-related downstream genes in the *flb27* mutant suggests that RISBZ1 acts as a negative regulator of UPR signaling pathway. Furthermore, RISBZ1 forms complexes with bZIP50 and bZIP60 in the nucleus under ER stress conditions, repressing their DNA binding affinities of downstream UPR genes (Figure 5). Additionally, overexpressing *RISBZ1* resulted in the down-regulation of UPR downstream genes in isolated rice protoplasts treated with 10 mM DTT (Figures 6B). These results strongly support the idea that RISBZ1 functions as a negative regulator of the UPR under ER stress conditions. Consistently, grains of the *bzip50 risbz1* and *bzip60 risbz1* double mutants were more floury than the *bzip50* and *bzip60* single mutants as well as the higher accumulation of BiP1 and PDIL1-1 proteins (Figures 6C-6J). However, in the *bzip50* or *bzip60* single mutant, the expression of *bZIP60* or *bZIP50* was highly induced (Figures 4A and 4C), suggesting a possible mutual compensational effect between the two arms of UPR signaling pathway. One possible explanation is that the ER homeostasis is disturbed in the *bzip60* mutant due to the accumulation of unfolded proteins, which may then activate IRE1 to promote the accumulation of bZIP50 and subsequent activation of the UPR. Therefore, it is plausible that many UPR related-genes in their single knockout lines showed up-regulation instead of down-regulation (Figures 4A and 4C).

It is worth noting that a previous report showed that the knockout mutant of *bZIP50* resulted in significantly elevated grain chalkiness (Yang et al., 2022), while in our study, grains of *bzip50-1/-2* exhibit only slight chalkiness (Supplemental Figure 10C). Besides, the grain phenotype of their *bZIP60* knockout mutant is also much more severe than *bzip60-1/-2* in our study (Supplemental Figure 10D; Yang et al., 2022). This discrepancy may be due to the different environments in which the plants were grown. The temperature in Wuhan city (N 29.6°-31.2°) during grain filling of ZH11 is much higher than that in Beijing city (N39.4°-41.6°), suggesting that RISBZ1, bZIP50 and bZIP60 play essential roles in the regulating high temperature-triggered ER

stress/UPR responses in rice. In support of this, we found that grain development in the *bzip50 risbz1* and *bzip60 risbz1* double mutants was more sensitive to high-temperature treatment, displaying severe floury and shrunken grains (Supplemental Figure 13). Besides, the grain phenotype of *bzip60* is much more severe than that of *bzip50* (Supplemental Figure 10, Yang et al., 2022; Zhou et al., 2022), indicating that bZIP60 plays a more predominant role than bZIP50 in the UPR pathway in rice. Moreover, our results together with previous studies demonstrate that both loss-of-function and overexpression of *bZIP50* and *bZIP60* disturbs the ER homeostasis, thereby activating the UPR and developing various degrees of grain chalkiness (Figures 4A-4D, Supplemental Figure 10; Yang et al., 2022). Therefore, appropriate expression levels of *bZIP50* and *bZIP60* could fine-tune the UPR, ensuring normal endosperm development and the production of low chalky grains.

Our haplotype analysis suggests that *RISBZ1*-Hap2 and *RISBZ1*-Hap6 have been retained in the *japonica* and *indica* subpopulation by positive selection, and exhibit a conspicuous tendency for northward and southward expansion, respectively (Supplemental Figure 14). These patterns suggest that *RISBZ1*-Hap2 and *RISBZ1*-Hap6 may facilitate the adaptation of rice to cold or heat environments, respectively, which needs further validation. Optimal haplotype combination of *bZIP50*, *bZIP60* and *RISBZ1* with appropriate expression levels should be explored and utilized to develop high-quality varieties resistant to ER or heat stress in future studies.

Previous studies and our new findings here demonstrate that *RISBZ1* plays pleiotropic roles during rice grain filling, especially under ER stress conditions (Figure 7). Under normal conditions, the nucleus-localized *RISBZ1* predominantly regulates the expression of SSP and starch biosynthesis-related genes to facilitate the rapid accumulation of dry matter in rice endosperm. bZIP50 and bZIP60 proteins are anchored to the ER membrane to avoid their excessively translocation into the nucleus, thereby maintaining appropriate chaperon levels for normal cellular function. However, ER stress conditions trigger the translocation of bZIP50 and bZIP60 from the ER to the nucleus to activate the expression of UPR downstream genes. In the nucleus, *RISBZ1* interacts with bZIP50 and bZIP60, leading to the transcriptional

repression of UPR signaling by blocking their binding affinities to the promoter regions of UPR genes. Interestingly, this interaction also inhibits the RISBZ1-mediated transcriptional activation of SSP genes and starch biosynthesis-related genes, which may lead to reduced accumulation of dry reserves. The mutual inhibition of gene expression mediated by the interaction of RISBZ1 with bZIP50 and bZIP60 may alleviate ER stress, but at the expense of diminished dry matter accumulation under detrimental conditions, such as high temperature during grain filling. Our results also offer a plausible explanation for the phenomenon that high temperature down-regulates the expression of SSRGs (Supplemental Figure 15, Zhang et al., 2018), except for the alternative splicing of *RISBZ1* (Xu et al., 2020). When RISBZ1 is knocked out, as the case of the *flo27* mutant, the inhibitory effect on bZIP50 and bZIP60 proteins is released, leading to a severe ER stress response as well as significantly reduced dry matter accumulation and the development of floury endosperm. Therefore, RISBZ1 functions cooperatively with bZIP50 and bZIP60 to balance grain filling and the ER stress response in rice.

In conclusion, this study uncovered an unusual function of RISBZ1 in the rice grain-filling process. The establishment of RISBZ1 as a negative regulator of the UPR signaling pathway provides new insight into the cellular mechanisms that enable rice grains to cope with ER stress. The identification of RISBZ1-mediated crosstalk between stress responses and grain filling has important implications for the improvement of crop yield and quality, especially in the context of increasing global populations and the challenges posed by global warming.

## METHODS

### Plant materials and growth conditions

The *flo27* mutant was obtained from a T-DNA mutant pool generated from rice *ssp. japonica* cv. Dongjin. All plants were grown in paddy fields at the Chinese Academy of Agricultural Sciences (Beijing, China) and Nanjing Agricultural University (Nanjing, China) under natural conditions with conventional management.

For high temperature treatment, wild type, *bzip50*, *bzip60*, *bzip50 risbz1* and *bzip60 risbz1* plants at the flowering stage were transferred to plant growth chambers under normal-temperature (28°C, 12 h light / 22°C, 12 h

dark) and high-temperature (35°C, 12 h light / 28°C, 12 h dark) conditions. At the mature stage, grains from different treatments were harvested and characterized for the phenotypes.

### **Measurement of total starch, amylose and protein content**

Rice grains were processed using a dehuller and ground into fine flour with a miller. Contents of total starch, amylose and protein were subsequently measured following the method outlined in a previous study (Lei et al., 2022).

### **Protein extraction and immunoblot analysis**

Protein extraction was performed as described by Takemoto et al. (2002), followed by SDS-PAGE and immunoblot assays as described by Wang et al. (2016). Synthetic peptides of AGPS2a, AGPL2, BEI, BEIIb, SSI, ISA1, GBSSI, GluA, GluB and Glb were used to generate specific polyclonal antibodies in rabbits by Yingji Biotech (<http://www.immunogen.com.cn/>) as previously described (Long et al., 2018). The anti-EF-1 $\alpha$  antibodies were purchased from Agrisera (AS10934).

### **Microscopy**

Scanning electron microscopy (SEM) was performed as described previously (Peng et al., 2014). Transverse sections of mature seeds were observed with a HITACHI S-3400N scanning electron microscope. To observe amyloplast morphology, transverse sections of developing endosperm (approximately 1-2 mm thick) of wild-type and *flo27* seeds were fixed overnight in 0.1 M phosphate buffer (pH 7.2) with 2% (v/v) glutaraldehyde and 2% (w/v) paraformaldehyde. Samples were embedded and sectioned as previously described (Kang et al., 2005). Semi-thin sections (1  $\mu$ m thick) were stained with I<sub>2</sub>-KI (0.5%) and subsequently examined under a light microscope (80i, Nikon). To assess the ultrastructure, developing seeds (12 DAF) were fixed for at least 12 h in 2.5% glutaraldehyde buffered with 0.2 M sodium phosphate buffer (pH 7.2), sectioned with an ultra-microtome (Power Tome-XL, RMC) and observed using a transmission electron microscope (H-7650, Hitachi).

### **Map-based cloning of *RISBZ1***

To map the *FLO27* locus, an F<sub>2</sub> population derived from the cross between the *flo27* mutant and an *indica* variety N22 was developed. A total of 1464

recessive individuals were used for fine mapping of *FLO27*. Primers used are listed in Supplemental Table 1.

### **Subcellular localization and BiFC assays**

For subcellular localization assays, the full-length amino acid sequences of *RISBZ1*, *bZIP50*, and *bZIP60* were fused to GFP under the control of two copies of the CaMV35S promoter in the pAN580-GFP transient expression vector. Rice protoplast preparation and transformation were performed as previously described (Chen et al., 2006). D53 (LOC\_Os11g01330) (Zhou et al., 2013) and mCherry-KDEL were used as nuclear and ER localization markers, respectively. To induce ER stress, protoplasts were treated with 10 mM DTT for 16 h. For BiFC assays, the coding sequence (CDS) of *RISBZ1* was amplified and cloned into the pYN vector, and the CDSs of *bZIP50* and *bZIP60* were amplified and cloned into the pYC vectors. *Nicotiana benthamiana* leaf transformation was performed as described previously (Kerppola, 2018). To induce ER stress, *N. benthamiana* leaves were treated with 2 mM DTT for 16 h after transfection. Fluorescence was observed using a confocal laser-scanning microscope (Zeiss LSM 780). Primers used are described in Supplemental Table 1.

### **Firefly luciferase complementation assays**

The CDSs of *bZIP60* and *RISBZ1* were cloned into pCAMBIA-nLUC, and the CDSs of *bZIP50* and *RISBZ1* were cloned downstream of C-Luc in pCAMBIA-cLUC. The plasmids were then transiently expressed in *N. benthamiana* leaves. To induce ER stress, the leaves were treated with 2 mM DTT for 16 h, between 24 and 48 h after transfection. The assays were performed as previously described (Chen et al., 2008). Primers used are described in Supplemental Table 1.

### **Yeast one-hybrid and yeast two-hybrid assays**

For Y1H assays, various regions of the *PDIL1-4*, *PDIL2-1*, *PDIL2-3*, *CRT*, *NEF*, *ERDJ3* and *BiP1* promoters were amplified and cloned into the pLacZi58 Y1H vector. Yeast strains were all grown on double dropout (SD/-Ura/-Trp) and X-Gal plates. For Y2H assays, the CDSs of *bZIP50* and *bZIP60* were cloned into pGADT7 (prey vector), while the CDS of *RISBZ1* was cloned into pGBKT7 (bait vector). These constructs were co-transformed into yeast

strain AH109 as described in the Matchmaker™ Gold Yeast Two-Hybrid System User Manual (Clontech Laboratories). Yeast strains were grown on double dropout (SD/-Leu/-Trp, DDO) and quadruple dropout (SD/-Leu/-Trp/-Ade/-His, QDO) plates containing 10 mM 3-AT (Sigma-Aldrich) to identify positive interactions. Primers used are described in Supplemental Table 1.

### **Electrophoretic mobility shift assay (EMSA)**

The full-length coding sequences of *RISBZ1*, *bZIP50* and *bZIP60* were amplified and inserted into the pMAL-c2X vector. MBP and MBP-RISBZ1 were expressed and purified from the *Escherichia coli* strain DE3 using amylose resin (NEB, E8021S) following the manufacturer's instructions. Biotin labeled DNA probes were synthesized by Invitrogen. DNA gel-shift assays were performed using a light-shift chemiluminescent EMSA Kit (Pierce, 20148) following the manufacturer's protocol. The relative intensities of shifted bands were calculated by the Image J software. Primers used are described in Supplemental Table 1.

### **Chromatin immunoprecipitation assay (ChIP)**

A synthetic peptide of bZIP60 (NYGEKGGSGNQGKEE) was injected into rabbits to generate the corresponding polyclonal antibodies at ABclonal Tech Co (Wuhan, China). The specificity of anti-OsbZIP60 polyclonal antibodies was determined by western blot analysis in Dongjin endosperm at 12 DAF.

ChIP assay was performed according to the previously described method (Duan *et al.*, 2019). Briefly, ~ 2 g developing endosperm at 12 DAF of Dongjin and *flo27* were ground into fine powder, fixed by formaldehyde and the nucleus was extracted. Chromatin was sonicated to fragments 200~500 bp in length and immunoprecipitated with specific anti-bZIP60 polyclonal antibodies. The recovered DNA was used as template for ChIP-qPCR and the fold enrichment was calculated as the ratio of IP to Input. Primers used are described in Supplemental Table 1.

### **Luciferase activity assays**

The promoter sequences (approximately 2.5 kb) of *PDIL1-1*, *BiP1*, *NEF*, *PDIL1-4*, *GluA2* and *AGPL3* were amplified and cloned into pGreenII 0800-LUC to generate reporter plasmids. The full-length CDSs of *RISBZ1*, *bZIP50* and *bZIP60* were amplified and cloned into the pCAMBIA1305 vector to

generate the effector plasmids. The plasmids were transiently expressed in *N. benthamiana* leaves by *Agrobacterium tumefaciens*-mediated transfection, and the luciferase activity was measured using the Dual-Luciferase Reporter Assay System (Promega, E2920). The ER stress induction was performed as described above. Primers used are described in Supplemental Table 1.

### **Pull-down assays**

For *in vitro* pull-down assays, the CDSs of *RISBZ1*, *bZIP50*, and *bZIP60* were cloned into pGEX4T-1 or pMAL-c2X vectors to generate plasmids carrying *RISBZ1-GST*, *bZIP50-MBP* and *bZIP60-MBP* fusions. GST- or *RISBZ1-GST*-coupled beads were used to capture *bZIP50-MBP* and *bZIP60-MBP* proteins. The pull-down assays were performed as previously described (Duan et al., 2019), and anti-MBP (NEB, E8038S) and anti-GST (MBL, PM013-7) antibodies at 1:5000 dilutions were used for detection. Primers used are described in Supplemental Table 1.

### **Generation of transgenic plants**

For complementation of the *flo27* phenotype, the 2-kb *RISBZ1* promoter region and its CDS were cloned into pCUbi1390 and then transformed into *flo27* to generate *RISBZ1* complementation lines.

To generate the *RISBZ1*, *bZIP50* and *bZIP60* knockout lines, a 20-bp gene-specific sequence was cloned into the CRISPR/Cas9 expression vector (Lei et al., 2014), and subsequently introduced into the calli of Dongjin. Positive transgenic individuals were identified by sequencing. All transgenic plants were generated using *Agrobacterium*-mediated transfection.

### **RNA extraction and quantitative RT-PCR**

Total RNA was extracted from different rice tissues using an RNA Prep Pure Kit (Zymo Research, D7003). RNA was reverse transcribed with the QuantiTect Reverse Transcription Kit (QIAGEN, 205314) following the manufacturer's protocol. RT-qPCR reactions were conducted using an ABI 7500 system with SYBR Premix Ex Taq (TAKARA, RR041A) according to the manufacturer's instructions. Gene expression levels were analyzed from three biological replicates using the relative quantification method (Livak et al., 2001) (Primer pairs were listed in Supplemental Table 1).

### **Haplotype, selection and evolutionary analysis**

Resequencing data for *RISBZ1* were obtained from in-house resequencing data and publicly available wild rice data (Jing et al., 2023). Haplotype classification of *RISBZ1* was performed using SNP variants from these datasets. The geographical distribution of *RISBZ1* haplotypes was annotated using the Maps R package (Rv4.3.2) under the GPL-2 license.

For selection analysis, sequence datasets encompassing the *RISBZ1* coding region and upstream and downstream 4 Mb regions were obtained from publicly available wild rice data (Jing et al., 2023). Nucleotide diversity ( $\pi$  values) for different subpopulations and the Fixation index ( $F_{ST}$ ) were calculated using a sliding window approach with a window size of 200 kb and a step of 20 kb via the Vcftools software (Danecek et al., 2011).

### **Quantification and statistical analysis**

All plant materials used for phenotypic evaluation, immunoblot and RT-qPCR analyses were grown simultaneously in the same conditions and time period with consistent management. All data are presented as means  $\pm$  SD and the statistical significance between control and experimental groups was determined by a Two-sided Students *t*-test ( $*P < 0.05$ ,  $**P < 0.01$ ) using the GraphPad Prism 8 software. The exact sample sizes, descriptions of control groups, quantification methods, and details of statistical analyses can be found in the figure legends. No data were excluded from analyses.

### **Data availability**

All study data are included in the article and/or supporting information. Genome sequence data from this study can be found in the GenBank/EMBL libraries under the following accession numbers: *RISBZ1*, LOC\_Os07g08420; *bZIP50*, LOC\_Os06g41770; *bZIP60*, LOC\_Os07g44950; *bZIP39*, LOC\_Os05g34050; *PDIL1-1*, LOC\_Os11g09280; *PDIL1-4*, LOC\_Os02g01010; *PDIL2-1*, LOC\_Os05g06430; *PDIL2-2*, LOC\_Os01g23740; *PDIL2-3*, LOC\_Os09g27830; *PDIL5-1*, LOC\_Os03g17860; *PDIL5-2*, LOC\_Os04g35290; *PDIL5-4*, LOC\_Os07g34030; *BiP1*, LOC\_Os02g02410; *BiP2*, LOC\_Os06g10990; *HSP70*, LOC\_Os02g48110; *HSP90*, LOC\_Os06g50300; *CNX*, LOC\_Os04g32950; *CRT*, LOC\_Os03g61670; *NEF*, LOC\_Os09g33780; *ERDJ3*, LOC\_Os05g06440; *Stt3a*, LOC\_Os04g57890; *UGT4*, LOC\_Os06g39260; *Derlin*, LOC\_Os03g63520; *GluA2*, LOC\_Os10g26060; *AGPL3*, LOC\_Os03g52460.

## FUNDING

This research was supported by the National Key Research and Development Program of China (2022YFD12000101), the Innovation Program of Chinese Academy of Agricultural Sciences, the “JBGS” Project of Seed Industry Revitalization in Jiangsu Province (JBGS(2021)008), the Natural Science Foundation of Jiangsu (BK20240192), the Fundamental Research Funds for the Central Universities (KYT2024005 and KYZZ2024005), and the earmarked fund for China Agriculture Research System (CARS-01-05). The work was also supported by the Key Laboratory of Biology, Genetics, and Breeding of *Japonica* Rice in Mid-lower Yangtze River, Ministry of Agriculture, P.R. China, and Jiangsu Collaborative Innovation Center for Modern Crop Production.

## AUTHOR CONTRIBUTIONS

J.M.W., Y.H.W. and Y.L.R. designed and conceived the research. Y.H.W. provided the *flo27* mutant and the mapping population. Q.S., E.C.D., R.N.J., H.X., C.W.G., W.T.L., X.K.J., R.B.C., Q.K.W., Y.P.Z., R.S.Z., H.Y.X., Y.P.Z., J.J.C., Y.F.F., Y.Z., Y.Z. and B.L.Z. performed the experiments. Q.S., E.C.D., R.N.J., H.X., C.W.G., W.T.L., X.T. and H.D. analyzed data. X.Y., L.Z., Y.L.T., X.L., S.J.L., X.P.G., C.L.L. and L.J. generated and cultivated the materials. E.C.D., Q.S. and R.N.J. wrote the paper. Y.H.W., Y.L.R. and J.M.W. revised the paper.

## ACKNOWLEDGEMENTS

We thank Yuanxin Yan at Nanjing Agricultural University for providing the maize *o2* mutant and its wild type.

## REFERENCES

- Bertolotti, A., Wang, X.Z., Novoa, I., Jungreis, R., Schlessinger, K., Cho, J.H., West, A.B., Ron, D.** (2001). Increased sensitivity to dextran sodium sulfate colitis in IRE1 beta-deficient mice. *J Clin Invest.* **107**:585-593.
- Cao, R.J., Zhao, S.L., Jiao, G.A., Duan, Y.Q., Ma, L.Y., Dong, N.N., Lu, F.F., Zhu, M.D., Shao, G.N., Hu, S.K., et al.** (2022). *Opaque3*, encoding a transmembrane bZIP transcription factor, regulates endosperm storage protein and starch biosynthesis in rice. *Plant Commun.* **3**:100463.

- Chen, E.W., Yu, H.Q., He, J., Peng, D., Zhu, P.P., Pan, S.X., Wu, X., Wang, J.C., Ji, C., Chao, Z.F., et al.** (2023). The transcription factors ZmNAC128 and ZmNAC130 coordinate with Opaque2 to promote endosperm filling in maize. *Plant Cell*. **35**:4066-4090.
- Chen, H.M., Zou, Y., Shang, Y.L., Lin, H.Q., Wang, Y.J., Cai, R., Tang, X.Y., Zhou, J.M.** (2008). Firefly luciferase complementation imaging assay for protein-protein interactions in plants. *Plant Physiol*. **146**:368-376.
- Chen, S.B., Tao, L.Z., Zeng, L.R., Vega-Sanchez, M.E., Umemura, K., Wang, G.L.** (2006). A highly efficient transient protoplast system for analyzing defence gene expression and protein-protein interactions in rice. *Mol Plant Pathol*. **7**:417-427.
- Danecek, P., Auton, A., Abecasis, G., Albers, C.A., Banks, E., DePristo, M.A., Handsaker, R.E., Lunter, G., Marth, G.T., Sherry, S.T., et al.** (2011). The variant call format and VCFtools. *Bioinformatics*. **27**:2156-8.
- Deng, Y., Humbert, S., Liu, J.X., Srivastava, R., Rothstein, S.J., Howell, S.H.** (2011). Heat induces the splicing by IRE1 of a mRNA encoding a transcription factor involved in the unfolded protein response in Arabidopsis. *Proc Natl Acad Sci USA*. **108**:7247-7252.
- Deng, Y.T., Wang, J.C., Zhang, Z.Y., Wu, Y.R.** (2020). Transactivation of *Sus1* and *Sus2* by Opaque2 is an essential supplement to sucrose synthase-mediated endosperm filling in maize. *Plant Biotechnol J*. **18**:1897-1907.
- Duan, E.C., Wang, Y.H., Li, X.H., Lin, Q.B., Zhang, T., Wang, Y.P., Zhou, C.L., Zhang, H., Jiang, L., Wang, J.L., et al.** (2019). OsSHI1 regulates plant architecture through modulating the transcriptional activity of IPA1 in rice. *Plant Cell* **31**:1026-1042.
- Fonseca, S.G., Ishigaki, S., Oslowski, C.M., Lu, S.M., Lipson, K.L., Ghosh, R., Hayashi, E., Ishihara, H., Oka, Y., Permutt, M.A., et al.** (2010). *Wolfram syndrome 1* gene negatively regulates ER stress signaling in rodent and human cells. *J Clin Invest*. **120**:744-755.
- Gao, H.B., Brandizzi, F., Benning, C., Larkin, R.M.** (2008). A membrane-tethered transcription factor defines a branch of the heat stress response in *Arabidopsis thaliana*. *Proc Natl Acad Sci USA*. **105**:16398-16403.

- Guo, X.M., Ronhovde, K., Yuan, L.L., Yao, B., Soundararajan, M.P., Elthon, T., Zhang, C., Holding, D.R.** (2012). Pyrophosphate-dependent fructose-6-phosphate 1-phosphotransferase induction and attenuation of *Hsp* gene expression during endosperm modification in quality protein maize. *Plant Physiol.* **158**:917-929.
- Han, X., Wang, Y.H., Liu, X., Jiang, L., Ren, Y.L., Liu, F., Peng, C., Li, J.J., Jin, X.M., Wu, F.Q., et al.** (2012). The failure to express a protein disulphide isomerase-like protein results in a floury endosperm and an endoplasmic reticulum stress response in rice. *J. Exp. Bot.* **63**:121-130.
- Harding, H.P., Zhang, Y.H., Ron, D.** (1999). Protein translation and folding are coupled by an endoplasmic-reticulum-resident kinase. *Nature* **398**:90-90.
- Hayashi, S., Takahashi, H., Wakasa, Y., Kawakatsu, T., Takaiwa, F.** (2013). Identification of a *cis*-element that mediates multiple pathways of the endoplasmic reticulum stress response in rice. *Plant J.* **74**:248-257.
- Hayashi, S., Wakasa, Y., Takahashi, H., Kawakatsu, T., Takaiwa, F.** (2012). Signal transduction by IRE1-mediated splicing of *bZIP50* and other stress sensors in the endoplasmic reticulum stress response of rice. *Plant J.* **69**:946-956.
- Hong, Z.H., Qing, T., Schubert, D., Kleinmanns, J.A., Liu, J.X.** (2019). BLISTER-regulated vegetative growth is dependent on the protein kinase domain of ER stress modulator IRE1A in *Arabidopsis thaliana*. *Plos Genet.* **15**:e1008563.
- Howell, S.H.** (2013). Endoplasmic reticulum stress responses in plants. *Annu Rev Plant Biol.* **64**:477-499.
- Iwata, Y., Koizumi, N.** (2012). Plant transducers of the endoplasmic reticulum unfolded protein response. *Trends Plant Sci.* **17**:720-727.
- Iwata, Y., Yoneda, M., Yanagawa, Y., Koizumi, N.** (2009). Characteristics of the nuclear form of the *Arabidopsis* transcription factor AtbZIP60 during the endoplasmic reticulum stress response. *Biosci Biotechnol Biochem.* **73**:865-869.
- Iwata, Y., Koizumi, N.** (2005). An *Arabidopsis* transcription factor, AtbZIP60, regulates the endoplasmic reticulum stress response in a manner unique to plants. *Proc Natl Acad Sci USA.* **102**:5280-5285.

- Iwawaki, T., Hosoda, A., Okuda, T., Kamigori, Y., Nomura-Furuwatari, C., Kimata, Y., Tsuru, A., Kohno, K.** (2001). Translational control by the ER transmembrane kinase/ribonuclease IRE1 under ER stress. *Nat Cell Biol.* **3**:158-164.
- Jing, C.Y., Zhang, F.M., Wang, X.H., Wang, M.X., Zhou, L., Cai, Z., Han, J.D., Geng, M.F., Yu, W.H., Jiao, Z.H., et al.** (2023). Multiple domestications of Asian rice. *Nat Plants.* **9**:1221-1235.
- Kang, H.G., Park, S., Matsuoka, M., An, G.H.** (2005). White-core endosperm *floury endosperm-4* in rice is generated by knockout mutations in the C-4-type pyruvate orthophosphate dikinase gene (*OsPPDKB*). *Plant J.* **42**:901-911.
- Kawakatsu, T., Yamamoto, M.P., Touno, S.M., Yasuda, H., Takaiwa, F.** (2009). Compensation and interaction between RISBZ1 and RPBF during grain filling in rice. *Plant J.* **59**:908-920.
- Kerppola, T.K.** (2008). Biomolecular fluorescence complementation (BiFC) analysis as a probe of protein interactions in living cells. *Annu Rev Biophys.* **37**:465-487.
- Lai, Y.S., Renna, L., Yarema, J., Ruberti, C., He, S.Y., Brandizzi, F.** (2018). Salicylic acid-independent role of NPR1 is required for protection from proteotoxic stress in the plant endoplasmic reticulum. *Proc Natl Acad Sci USA.* **115**:E5203-E5212.
- Lei, J., Teng, X., Wang, Y.F., Jiang, X.K., Zhao, H.H., Zheng, X.M., Ren, Y.L., Dong, H., Wang, Y.L., Duan, E.C., et al.** (2022). Plastidic pyruvate dehydrogenase complex E1 component subunit Alpha1 is involved in galactolipid biosynthesis required for amyloplast development in rice. *Plant Biotechnol J.* **3**:437-453.
- Lei, Y., Lu, L., Liu, H.Y., Li, S., Xing, F., Chen, L.L.** (2014). CRISPR-P: a web tool for synthetic single-guide RNA design of CRISPR-system in plants. *Mol Plant* **7**:1494-1496.
- Li, C.B., Qi, W.W., Liang, Z., Yang, X., Ma, Z.Y., Song, R.T.** (2020). A SnRK1-ZmRFWD3-Opaque2 signaling axis regulates diurnal nitrogen accumulation in maize seeds. *Plant Cell* **32**:2823-2841.
- Lin, J.H., Walter, P., Yen, T.S.** (2008). Endoplasmic reticulum stress in disease pathogenesis. *Annu Rev Pathol.* **3**:399-425.

- Liu, J.X., Srivastava, R., Che, P., Howell, S.H.** (2007a). Salt stress responses in *Arabidopsis* utilize a signal transduction pathway related to endoplasmic reticulum stress signaling. *Plant J.* **51**:897-909.
- Liu, J.X., Srivastava, R., Che, P., Howell, S.H.** (2007b). An endoplasmic reticulum stress response in *Arabidopsis* is mediated by proteolytic processing and nuclear relocation of a membrane-associated transcription factor, bZIP28. *Plant Cell.* **19**:4111-4119.
- Liu, J.X., Howell, S.H.** (2010a). bZIP28 and NF-Y transcription factors are activated by ER Stress and assemble into a transcriptional complex to regulate stress response genes in *Arabidopsis*. *Plant Cell* **22**:782-796.
- Liu, J.X., Howell, S.H.** (2010b). Endoplasmic reticulum protein quality control and its relationship to environmental stress responses in plants. *Plant Cell* **22**:2930-2942.
- Livak, K.J., Schmittgen, T.D.** (2001). Analysis of relative gene expression data using real-time quantitative PCR and the  $2^{-\Delta\Delta CT}$  method. *Methods* **25**:402-408.
- Long, W.H., Wang, Y.L., Zhu, S.S., Jing, W., Wang, Y.H., Ren, Y.L., Tian, Y.L., Liu, S.J., Liu, X., Chen, L.M., et al.** (2018). FLOURY SHRUNKEN ENDOSPERM1 connects phospholipid metabolism and amyloplast development in rice. *Plant Physiol.* **177**:698-712.
- Lu, S.J., Yang, Z.T., Sun, L., Sun, L., Song, Z.T., Liu, J.X.** (2012). Conservation of IRE1-regulated *bZIP74* mRNA unconventional splicing in rice (*Oryza sativa* L.) involved in ER stress responses. *Mol. Plant* **5**:504-514.
- Meng, Z., Ruberti, C., Gong, Z.Z., Brandizzi, F.** (2017). CPR5 modulates salicylic acid and the unfolded protein response to manage tradeoffs between plant growth and stress responses. *Plant J.* **89**:486-501.
- Mizuno, T., Masuda, Y., Irie, K.** (2015). The *Saccharomyces cerevisiae* AMPK, Snf1, negatively regulates the Hog1 MAPK pathway in ER stress response. *Plos Genet.* **11**:e1005491.
- Nagashima, Y., Mishiba, K., Suzuki, E., Shimada, Y., Iwata, Y., Koizumi, N.** (2011). *Arabidopsis* IRE1 catalyses unconventional splicing of *bZIP60* mRNA to produce the active transcription factor. *Sci Rep.* **1**:29

- Nakamura, D., Tsuru, A., Ikegami, K., Imagawa, Y., Fujimoto, N., Kohno, K.** (2011). Mammalian ER stress sensor IRE1 beta specifically down-regulates the synthesis of secretory pathway proteins. *FEBS Lett.* **585**:133-138.
- Nawkar, G.M., Kang, C.H., Maibam, P., Park, J.H., Jung, Y.J., Chae, H.B., Chi, Y.H., Jung, I.J., Kim, W.Y., Yun, D.J., et al.** (2017). HY5, a positive regulator of light signaling, negatively controls the unfolded protein response in Arabidopsis. *Proc Natl Acad Sci USA.* **114**:2084-2089.
- Onodera, Y., Suzuki, A., Wu, C.Y., Washida, H., Takaiwa, F.** (2001). A rice functional transcriptional activator, RISBZ1, responsible for endosperm-specific expression of storage protein genes through GCN4 motif. *J Biol Chem.* **276**:14139-14152.
- Oono, Y., Wakasa, Y., Hirose, S., Yang, L.J., Sakuta, C., Takaiwa, F.** (2010). Analysis of ER stress in developing rice endosperm accumulating  $\beta$ -amyloid peptide. *Plant Biotechnol J.* **8**:691-718.
- Peng, C., Wang, Y.H., Liu, F., Ren, Y.L., Zhou, K.N., Lv, J., Zheng, M., Zhao, S.L., Zhang, L., Wang, C.M., et al.** (2014). *FLOURY ENDOSPERM6* encodes a CBM48 domain-containing protein involved in compound granule formation and starch synthesis in rice endosperm. *Plant J.* **77**:917-930.
- Pu, Y., Ruberti, C., Angelos, E.R., Brandizzi, F.** (2019). AtIRE1C, an unconventional isoform of the UPR master regulator AtIRE1, is functionally associated with AtIRE1B in Arabidopsis gametogenesis. *Plant Direct.* **3**:e00187.
- Qiao, Z.Y., Qi, W.W., Wang, Q., Feng, Y.N., Yang, Q., Zhang, N., Wang, S.S., Tang, Y.P., Song, R.T.** (2016). ZmMADS47 regulates zein gene transcription through interaction with Opaque2. *Plos Genet.* **12**:e1005991.
- Ron, D., Walter, P.** (2007). Signal integration in the endoplasmic reticulum unfolded protein response. *Nat Rev Mol Cell Bio.* **8**:519-529.
- Takemoto, Y., Coughlan, S.J., Okita, T.W., Satoh, H., Ogawa, M., Kumamaru, T.** (2002). The rice mutant *esp2* greatly accumulates the glutelin precursor and deletes the protein disulfide isomerase. *Plant Physiol.* **128**:1212-1222.
- Vitale, A., Boston, R.S.** (2008). Endoplasmic reticulum quality control and the unfolded protein response: insights from plants. *Traffic* **9**:1581-1588.

- Wang, J., Chen, Z.C., Zhang, Q., Meng S.S., Wei, C.X.** (2020). The NAC transcription factor OsNAC20 and OsNAC26 regulate starch and storage protein synthesis. *Plant Physiol.* **184**:1775-1791.
- Wang, J.C., Xu, H., Zhu, Y., Liu, Q.Q., Cai, X.L.** (2013). OsbZIP58, a basic leucine zipper transcription factor, regulates starch biosynthesis in rice endosperm. *J Exp Bot.* **64**:3453-3466.
- Wang, Y.H., Liu, F., Ren, Y.L., Wang, Y.L., Liu, X., Long, W.H., Wang, D., Zhu, J.P., Zhu, X.P., Jing, R.N., et al.** (2016). GOLGI TRANSPORT 1B regulates protein export from the endoplasmic reticulum in rice endosperm cells. *Plant Cell* **28**:2850-2865.
- Wu, J.H., Zhu, C.F., Pang, J.H., Zhang, X.R., Yang, C.L., Xia, G.X., Tian, Y.C., He, C.Z.** (2014). OsLOL1, a C2C2-type zinc finger protein, interacts with OsbZIP58 to promote seed germination through the modulation of gibberellin biosynthesis in *Oryza sativa*. *Plant J.* **80**:1118-1130.
- Xu, H., Li, X.F., Zhang, H., Wang, L.C., Zhu, Z.G., Gao, J.P., Li, C.S., Zhu, Y.** (2020). High temperature inhibits the accumulation of storage materials by inducing alternative splicing of *OsbZIP58* during filling stage in rice. *Plant Cell Environ.* **43**:1879-1896.
- Yamamoto, M.P., Onodera, Y., Touno, S.M., Takaiwa, F.** (2006). Synergism between RPBF Dof and RISBZ1 bZIP activators in the regulation of rice seed expression genes. *Plant Physiol.* **141**:1694-1707.
- Yang, W.P., Xu, P.K., Zhang, J.C., Zhang, S., Li, Z.W., Yang, K., Chang, X.Y., Li, Y.B.** (2022). OsbZIP60-mediated unfolded protein response regulates grain chalkiness in rice. *J Genet Genomics* **49**:414-426.
- Yu, A.M., Li, P., Tang, T., Wang, J.C., Chen, Y., Liu, L.** (2015). Roles of Hsp70s in stress responses of microorganisms, plants, and animals. *Biomed Res Int.* **2015**:510319.
- Zhang, H., Xu, H., Feng, M.J., Zhu, Y.** (2018) Suppression of OsMADS7 in rice endosperm stabilizes amylose content under high temperature stress. *Plant Biotechnol J.* **16**:18-26.
- Zhang, Z.Y., Zheng, X.X., Yang, J., Messing, J., Wu, Y.R.** (2016). Maize endosperm-specific transcription factors O2 and PBF network the regulation of protein and starch synthesis. *Proc Natl Acad Sci USA.* **113**:10842-10847.

Zhou, F., Lin, Q.B., Zhu, L.H., Ren, Y.L., Zhou, K.N., Shabek, N., Wu, F.Q., Mao, H.B., Dong, W., Gan, L., et al. (2013). D14-SCF<sup>D3</sup>-dependent degradation of D53 regulates strigolactone signalling. *Nature* **504**:406-410.

Zhou, Y.F., Qing, T., Shu, X.L., Liu, J.X. (2022). Unfolded protein response and storage product accumulation in rice grains. *Seed Biol.* **1**:4.

### Figure legends:

#### Figure 1. Mutation of *FLO27* results in abnormal grain development.

**(A and B)** Appearance of mature grains from Dongjin (A) and *flo27* (B). Bars = 2.5 mm. **(C and D)** Transverse sections of mature grains from Dongjin (C) and *flo27* (D). Bars = 0.4 mm. **(E-H)** Scanning electron microscopy (SEM) images of transverse sections of Dongjin (E and G) and *flo27* (F and H) grains. Bars = 0.4 mm in (E) and (F), 10  $\mu$ m in (G) and (H). **(I and J)** Semithin sections of developing endosperm from Dongjin (I) and *flo27* (J) at 12 days after flowering (DAF). Bars = 20  $\mu$ m. **(K and L)** Transmission electron microscopic (TEM) analysis of developing endosperm from Dongjin (K) and *flo27* (L) at 12 DAF. PBI (blue arrowhead), protein body I; PBII (red arrowhead). Bars = 1  $\mu$ m. **(M)** Gene structure of *ORF13* (*LOC\_Os07g08420*) and the mutation site in the *flo27* mutant. Black boxes represent exons and lines between them indicate introns. ATG and TAG represent the start and stop codons, respectively. A 188-bp insertion in the last exon of *ORF13* in the *flo27* mutant results in premature translational termination. Asterisk represents stop codon in *flo27*. **(N)** Mature grain appearance of Dongjin, *flo27* and the representative complemented transgenic line (Com). The upper and lower panels represent the whole morphology and cross sections of mature grains from Dongjin, *flo27* and the complemented transgenic line (Com), respectively. Bars = 1 mm. **(O)** SDS-PAGE profiles of storage proteins in mature grains of Dongjin, *flo27* and complemented transgenic line (Com). pGT, proglutelins;  $\alpha$ GT, glutelin acidic subunits;  $\alpha$ Glb,  $\alpha$ -globulin;  $\beta$ GT, glutelin basic subunits; Pro, prolamins. Molecular weights of proteins (kDa) are indicated on the left.

#### Figure 2. Malfunction of *RISBZ1* results in ER stress.

**(A and B)** KEGG and GO analysis of the transcriptome sequencing data for the developing endosperm of *flo27*. The ER stress-related pathway and molecular functions of the enriched DEGs are highlighted in red. **(C-F)** RT-

qPCR analysis of the expression of genes coding for chaperones (C), including BiPs (binding proteins), PDILs (protein disulfide isomerase-like enzymes), HSPs (heat shock proteins), CNX (calnexin), CRT (calreticulin), co-chaperones (D), including ERDJ3 (ER-localized DnaJ family member 3), NEF (nucleotide exchange factor), Stt3A (STT3 oligosaccharyl transferase complex catalytic subunit A), UGT4 (UDP-glucose transferase 4), membrane-associated bZIP transcription factors (E), and the ERAD related protein Derlin and the programmed cell death (PCD) markers NPR1 (NON-EXPRESSOR OF PATHOGENESIS-RELATED GENES 1) (F). Data represent means  $\pm$  SD ( $n = 3$ ). The asterisks indicate statistical significance between *flo27* and Dongjin, as determined by a Student's *t*-test ( $n = 3$ ,  $**P < 0.01$ ). **(G)** Immunoblot analysis detecting the accumulation of BiP1 and PDIL1-1 chaperone proteins in mature grains of Dongjin and *flo27*. EF-1 $\alpha$  was used as a loading control. Molecular weights of proteins (kDa) are indicated on the left.

**Figure 3. RISBZ1 physically interacts with bZIP50 and bZIP60.**

**(A)** Subcellular localization of bZIP50 and bZIP60 in Dongjin and *flo27* protoplasts with or without 10 mM DTT treatment. mCherry-KDEL was used as the ER marker. Bars = 10  $\mu$ m. **(B)** Both bZIP50 and bZIP60 interacted with RISBZ1 in yeast two-hybrid assay. pGADT7 and pGBKT7 were used as the negative controls. 10 mM 3-AT was supplied to inhibit the auto-activation activity of RISBZ1 in yeast cells. **(C)** *In vitro* pull-down assay showing RISBZ1 interacted with bZIP50 and bZIP60. MBP-bZIP50 and MBP-bZIP60 were pulled down by RISBZ1 expressed as glutathione S-transferase (GST) fusion protein as detected by immunoblotting using anti-MBP antibody. GST protein was used as a negative control. The symbols “-” and “+” indicate the absence and presence of the corresponding proteins, respectively. Molecular weights of proteins (kDa) are indicated on the left. **(D)** Firefly LCI assay to detect physical interactions between RISBZ1 and bZIP50 (upper panel) and bZIP60 (lower panel) in leaf epidermal cells of *N. benthamiana* treated with 2 mM DTT. Colored scale bars indicate the luminescence intensity of CPS (count per second). nLUC, N terminus of LUC; cLUC, C terminus of LUC. The unrelated D53 protein with the same subcellular location was used as the negative control. **(E)** BiFC assay showing RISBZ1 interacts with bZIP50 and bZIP60 only in tobacco leaf epidermal cells treated with 2 mM DTT. Scale bars = 20

µm. YN and YC were used as the negative controls. BF, bright field. Merged, merged images of the GFP channel and bright field.

**Figure 4. bZIP50 and bZIP60 directly regulates UPR downstream genes.**

**(A)** RT-qPCR analysis of the expression of UPR-related genes between Dongjin and *bzip50-1*. Data represent means  $\pm$  SD ( $n = 3$ ). Asterisks indicate significant difference according to Student's *t*-test at  $**P < 0.01$ . **(B)** Immunoblot analysis showing the accumulation of BiP1 and PDIL1-1 chaperone proteins in mature grains of Dongjin and *bzip50-1*. EF-1 $\alpha$  was used as a loading control. Molecular weights of proteins (kDa) are indicated on the left. **(C)** RT-qPCR analysis of the expression of UPR-related genes between Dongjin and *bzip60-1*. Data represent means  $\pm$  SD ( $n = 3$ ). Asterisks indicate significant difference according to Student's *t*-test at  $**P < 0.01$ . **(D)** Immunoblot analysis showing the accumulation of BiP1 and PDIL1-1 chaperone proteins in mature grains of Dongjin and *bzip50-1*. EF-1 $\alpha$  was used as a loading control. Molecular weights of proteins (kDa) are indicated on the left. **(E)** Detection of interactions between bZIP50, bZIP60 and the chimeric promoters of UPR-related genes by Y1H analyses. The blue yeast colonies indicate positive interactions. pB42AD was used as the negative control. **(F)** Schematic representation of the effector and reporter constructs. Full-length coding regions of *bZIP50* and *bZIP60* under the control of the double 35S promoter were used as the effectors. The Firefly luciferase gene *LUC* driven by the *PDIL1-4* and *NEF* promoters and the Renilla luciferase gene *Ren* driven by the 35S promoter were used as the reporter and internal control, respectively. d35S, double 35S promoter. **(G)** Luciferase reporter assay showing that bZIP50 and bZIP60 activate the expression of *PDIL1-4* and *NEF* in rice protoplasts. Relative LUC activity was calculated by LUC/Ren and normalized to that of vector control (GFP) which was set as 1. Data are presented as means  $\pm$  SD ( $n = 3$ ). Asterisks indicate significant difference according to Student's *t*-test at  $**P < 0.01$ .

**Figure 5. RISBZ1 and bZIP50/60 repress the transcriptional activities of each other.**

**(A and B)** Luciferase reporter assay shows that RISBZ1 represses the transcriptional activation activities of bZIP60 on *BiP1* (A) and *PDIL1-1* (B) promoters in rice protoplasts. Relative LUC activity was calculated by

LUC/Ren and normalized to that of empty vector (GFP) control which was set to 1. Values are presented as means  $\pm$  SD ( $n = 3$ ). Bars with different letters are significantly different from each other ( $P < 0.05$ ). **(C and D)** EMSAs showing that RISBZ1-bZIP60 interaction reduces the DNA binding activity of bZIP60 to the promoter regions of *BiP1* (C) and *PDIL1-1* (D). The triangles indicate increasing amounts of RISBZ1 proteins. MBP protein was used as the negative control. The symbols “-” and “+” represent the absence and presence of the corresponding proteins, respectively. The shifted bands and free probes are indicated by arrows and arrowheads, respectively. The relative intensities of shifted bands are indicated below each band. **(E and F)** Luciferase reporter assay showing that bZIP50/60 repress the transcriptional activation activity of RISBZ1 on *GluA2* (E) and *AGPL3* (F) promoters in rice protoplasts. Relative LUC activity was calculated by LUC/Ren and normalized to that of empty vector (GFP) control which was set to 1. Values are presented as means  $\pm$  SD ( $n = 3$ ). Bars with different letters are significantly different from each other ( $P < 0.05$ ). **(G to J)** EMSAs showing that the RISBZ1-bZIP50/60 interaction reduce the DNA binding activity of RISBZ1 to the promoter regions of *GluA2* (G and H) and *Waxy* (I and J). The triangles indicate increasing amounts of bZIP50 or bZIP60 proteins. MBP protein was used as the negative control. The symbols “-” and “+” represent the absence and presence of the corresponding proteins, respectively. The shifted bands and free probes are indicated by arrows and arrowheads, respectively. The relative intensities of shifted bands are indicated below each band. **(K)** ChIP-qPCR assays showing that bZIP60 is more enriched in the promoter regions of UPR genes in *flo27* compared to Dongjin. DNAs precipitated from developing endosperm of Dongjin and *flo27* by anti-bZIP60 specific polyclonal antibodies were subjected to ChIP-qPCR analysis. The fold enrichment was calculated as IP/Input. NS, no significance. Values are presented as means  $\pm$  SD, and the statistically significant differences were determined by Students *t*-test ( $n = 3$ ,  $**P < 0.01$ ).

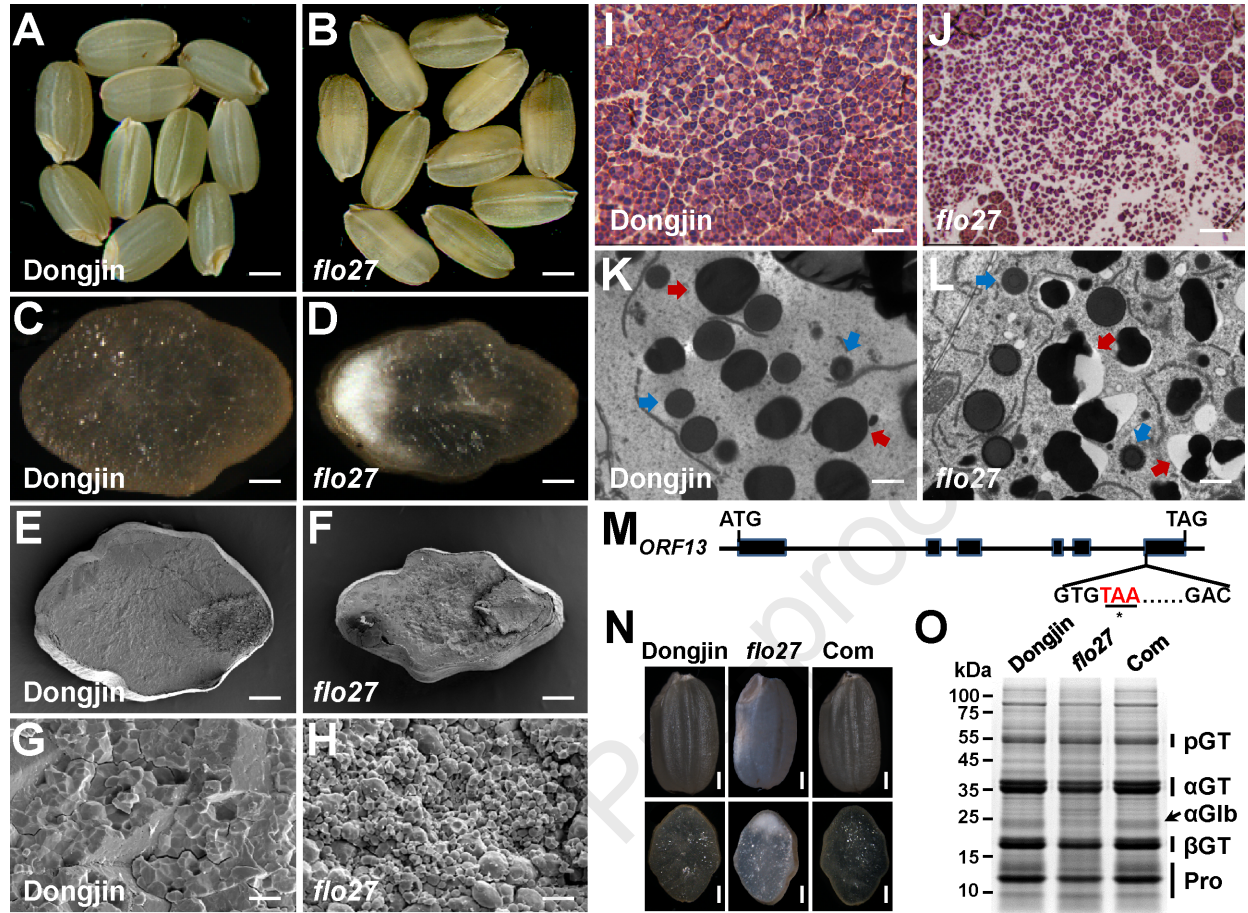
**Figure 6. RISBZ1 functions as a negative regulator of the UPR under ER Stress conditions.**

**(A)** Expression level of *RISBZ1* in developing grains of Dongjin and *bzip60* at 12 DAF. **(B)** RT-qPCR analysis of the expression of genes coding for

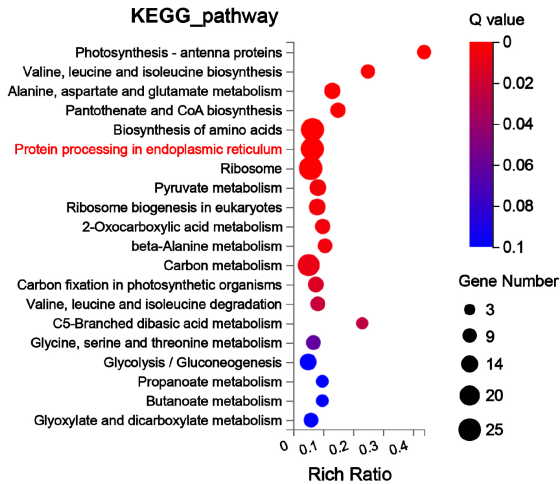
chaperones, co-chaperones, membrane-associated bZIP transcription factors in rice protoplasts treated with 10 mM DTT. **(C and D)** Morphology of mature grains of Dongjin, *bzip50*, *bzip60*, *bzip50 risbz1* and *bzip60 risbz1* mutants. Bars = 1 mm. **(E and F)** Grain chalkiness degrees of mature grains from Dongjin, *bzip50*, *bzip60*, *bzip50 risbz1* and *bzip60 risbz1* mutants. **(G and H)** Mature grain weights of Dongjin, *bzip50*, *bzip60*, *bzip50 risbz1* and *bzip60 risbz1* mutants. **(I and J)** Immunoblot analysis showing the accumulation of BiP1 and PDIL1-1 chaperone proteins in mature grains of Dongjin, *bzip50*, *bzip60*, *bzip50 risbz1* and *bzip60 risbz1* mutants. EF-1 $\alpha$  was used as a loading control. Molecular weights of proteins (kDa) are indicated on the left. Data represent means  $\pm$  SD (n = 3). Asterisks indicate significant difference according to Student's *t*-test at  $**P < 0.01$ . Bars with different letters are significantly different from each other ( $P < 0.05$ ).

**Figure 7. Proposed working model for the function of RISBZ1 in the grain-filling and ER stress signaling pathways.**

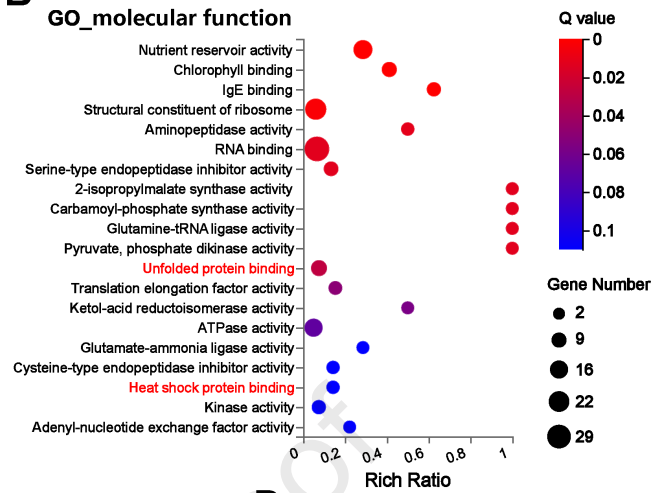
Under normal conditions, RISBZ1 primarily activates the expression of genes related to starch and storage protein synthesis. Under ER stress, bZIP50 and bZIP60 translocate from the ER to the nucleus to activate the UPR signaling pathway. In the nucleus, RISBZ1 interacts with the translocated bZIP50 and bZIP60 proteins to repress their DNA-binding activity, thereby downregulating the expression of UPR-related genes. This repression occurs at the expense of reduced transcription of starch and storage protein synthesis-related genes. Thus RISBZ1 alleviates ER stress at the cost of dry matter accumulation, maintaining a balance between grain-filling and adaptation to environment stress.



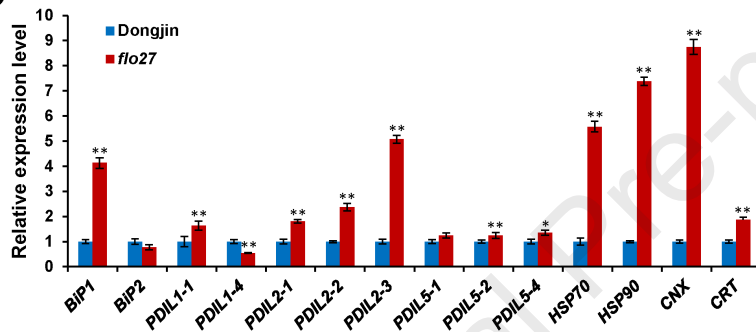
A



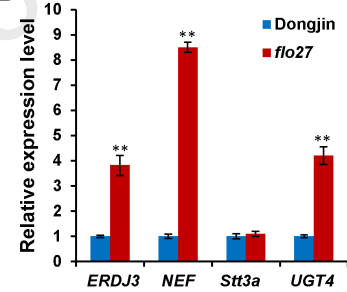
B



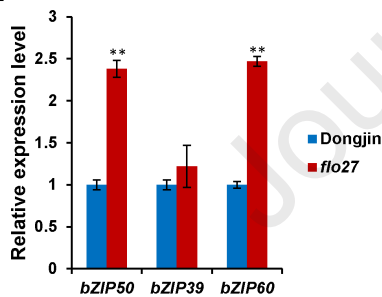
C



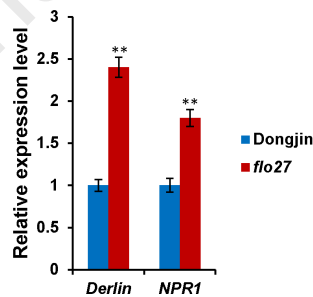
D



E



F



G

